Sorted cell microarrays as platforms for high-content informational bioassays†

Emily J. Anglin,[ab] Carolyn Salisbury,[c] Sheree Bailey,[de] Maryam Hor,[c] Peter Macardle,[de] Michael Fenech,*[c] Helmut Thissen[bf] and Nicolas H. Voelcker*[ab]

Received 9th July 2010, Accepted 9th September 2010
DOI: 10.1039/c0lc00185f

We report on surface-engineered microarrays that provide *in situ* cell sorting, localization, and immobilization of various subsets of human primary lymphocytes, followed by an on-chip bioassay for ionizing-radiation-induced cytogenetic damage. The microarray format eliminates the necessity of separating cell sub-populations by alternative means (such as fluorescence- or magnetic-activated cell sorting) prior to performing informational bioassays. To exemplify the potential of this on-chip cytometry approach, we have integrated the cytokinesis-block micronucleus cytome (CBMNcyt) assay with the microarray platform for analysis of the chromosome damage profile of specific subsets of human peripheral lymphocytes. Microarray results were compared with data obtained from the traditional CBMNcyt assay on heterogeneous lymphocyte populations, and with flow cytometry data. Our results suggest that cytogenetic damage caused by ionizing radiation is not uniformly distributed across all lymphocytes subsets, but rather concentrated in specific subsets. The salient features of our approach are that it requires very small volumes of reagents, allows sorting of lymphocyte subsets *in situ*, increases parallelism of cell assays and is amenable to high content microscopy analysis. The on-chip cytometry format opens new vistas for advanced cell-based assays, potentially bringing to light important information which remains hidden with conventional assays and hence engendering new discoveries in cell biology.

Introduction

New platform technologies allowing the study of specific cells within a heterogeneous population can enhance our fundamental understanding of cellular function and fuel the development of targeted therapies and more sensitive diagnostic medical assays. Amongst the emerging technology platforms, biochips are particularly valuable for diagnostic technologies since they are conducive to screening large numbers of cellular events at sub-cellular resolution or numerous patients simultaneously. Moreover, on-chip diagnostic technologies would be of benefit in point-of-care testing and in remote areas of the world provided that portable and miniaturized read-out tools are developed.

With the recent advent of cell-based microarrays,[1–5] one can now fabricate and study a multitude of cell microenvironments in parallel using only minimal amounts of reagents.[6–8] This high throughput approach is in stark contrast to conventional plating methods used routinely in cell biology. Examples for the successful demonstration of cell microarrays include probing stem cell isolation or differentiation in response to various biological and synthetic materials in high throughput.[9–14] Furthermore, the capacity for translation into clinical applications has been demonstrated recently by using cell microarrays as a diagnostic tool for leukemia and lymphoma profiling[15,16] as well as in HIV monitoring.[17]

A dynamic new field of research in preventative health is based on the development of new high throughput methods for studying effects of cyto- and genotoxins. The loss or gain of chromosomes, chromosome deletions, and chromosome rearrangements are amongst the most common causes of genetic disorders and, in particular, are potent catalysts for cancer development.[18] In terms of biodosimetry, it is well understood that cytogenetic damage occurs upon exposure to ionizing radiation in a dose dependent fashion.[19] Whether the genetic damage is uniformly distributed across all cellular subtypes or if it is more selectively featured in a particular cell type remains an open, yet important question that has significant implications for accurate dose–exposure assessment. Analysis of DNA damage amongst specific cell subsets would require costly and time-intensive cell separation, for example by means of fluorescence-activated cell sorting (FACS) or magnetic-activated cell sorting (MACS).[20] In comparison, an on-chip cytometer would potentially yield enhancement in selectivity, sensitivity, parallelism, analysis time and cost, significantly increasing the diagnostic value. Moreover, with the development of several high content screening microscope systems, the analytical process can be automated and the

[a]*School of Chemical and Physical Sciences, Flinders University, GPO Box 2100, Bedford Park, SA, 5042, Australia. E-mail: Nico.Voelcker@flinders.edu.au*
[b]*CSIRO Food Futures Flagship, Riverside Corporate Park 5 Julius Avenue, North Ryde, NSW, 2113, Australia*
[c]*CSIRO Food and Nutritional Sciences, PO Box 10041, Adelaide, SA, 5000, Australia. E-mail: Michael.Fenech@csiro.au*
[d]*Department of Immunology, Allergy and Arthritis, School of Medicine, Flinders University, Bedford Park, SA, 5042, Australia*
[e]*SA Pathology, 14 Rundle Mall, Adelaide, SA, 5000, Australia*
[f]*CSIRO Molecular and Health Technologies, Bayview Avenue, Clayton, VIC, 3168, Australia*
† Electronic supplementary information (ESI) available: FACS and on-chip separation methods and techniques. See DOI: 10.1039/c0lc00185f

high throughput potential of these platforms can be duly realized.[21–23]

The CBMNcyt assay is routinely applied as a reliable method to study genomic instabilities. It involves the detection and quantification of specific biomarkers of chromosome damage (micronuclei (MNi), nucleoplasmic bridges and nuclear buds) that form during mitosis and are expressed during anaphase.[18] In the CBMNcyt assay, cells that can express these biomarkers are those that have completed nuclear division and are accumulated as binucleated cells (BiN) after blocking cytokinesis using cytochalasin-B.[24] The presence of MNi within a BiN cell during nuclear division is indicative of chromosomal fragments or whole chromosomes that are malsegregated during anaphase. MNi have been associated with Alzheimer's disease,[25,26] Parkinson's disease,[26] lung cancer,[27] breast cancer[28] and several other adverse medical conditions.[29,30] Proper characterization and quantification of these biomarkers within various cell subsets would enhance the diagnostic value of the CBMNcyt assay and spur therapeutic advances, particularly if different cell subsets vary substantially in susceptibility to genotoxic agents or accelerated senescence.

By integrating a cell-based microarray allowing *in situ* cell separation and phenotypic studies of specific subpopulations of human peripheral lymphocytes with the CBMNcyt assay, we were able to identify subtypes which are more susceptible to DNA damage. We scored lymphocyte subsets for the formation of the MNi biomarker of DNA damage in BiN cells, which is the best validated biomarker within the CBMNcyt assay for studies relating to radiation biodosimetry.[31]

A surface-engineered coating was developed for cell microarrays based on allylamine plasma polymerization and subsequent spin-coating of random copolymers of glycidyl methacrylate (GMA) and poly(ethylene glycol)methacrylate (PEGMA). This background coating provided an epoxy functional group suitable for the covalent anchoring of arrayed capture probes and, at the same time, a non-fouling surface between printed spots discouraging non-specific cell attachment.[32,33] A robotic spotter was used for dispensing nanolitre volumes of monoclonal antibodies for capture of subpopulations of B and T cell lymphocytes and creating spots in a size range optimal for the desired bioassays. We have established techniques for separating lymphocytes stimulated by phytohaemagglutinin (PHA), an agent used to induce cell division in primary lymphocytes, and blocking cytokinesis with cytochalasin B (Cyto-B) to once-divided BiN cells, which are the cells that can express MNi. Heterogeneous populations of cells were then sorted and attached on the monoclonal capture antibody microarray platform. We have developed cell preparation and staining methods that allow for fluorescence and bright field analysis, and in particular, analysis of chromosome damage *via* scoring of relevant biomarkers in the CBMNcyt assay.

Experimental methods

Fabrication of microarray substrates

Partially frosted glass slides (Biolab) were surface-modified as described previously.[33,34] Briefly, glass slides were first coated with an allylamine (Aldrich, 98% purity) plasma polymer (ALAPP) using radio frequency glow discharge deposition in a custom-built reactor defined by a height of 35 cm and a diameter of 17 cm. The lower and upper electrodes were both circular, with a diameter of 10.5 cm and separation of 16 cm. Samples were placed on the lower electrode. Plasma polymer coatings were deposited using a frequency of 200 kHz, a power of 20 W, an initial monomer pressure of 0.200 mbar and a treatment time of 25 s.

Freshly ALAPP coated glass slides were subsequently spin coated with a 2.5 (w/v) copolymer solution in dioxane containing a crosslinker. The copolymer was freshly synthesized from poly(ethylene glycol)methyl ether methacrylate (PEGMA, Aldrich, M_w 475) and glycidyl methacrylate (GMA, Fluka) in dioxane (BDH Chemicals) in a 1 : 1 (w/w) ratio using 2,2′-azobisisobutyronitrile (AIBN, Aldrich) as an initiator. 0,0′-Bis (2-aminoethyl)poly(ethylene glycol) (PEG diamine, M_w 3400, Fluka) was used as a crosslinker in the spin coating solution at a concentration of 0.2% (w/v). Spin-coating was performed at 5000 rpm for 30 s after placing ALAPP coated glass slides on the spin coater (WS-400B-6NPP/Lite, Laurell Technologies Corporation) and covering the entire surface with the solution containing the copolymer and the crosslinker. After spin coating, the remaining solvent was removed in a vacuum.

Preparation of antibody microarrays

Prior to antibody printing, the PEGMA/GMA copolymer coated glass slides were soaked in sterile Dulbecco's phosphate buffered saline solution (PBS) for 1 h at 37 °C, rinsed with sterile MilliQ water and dried under ambient conditions. CD45, CD4, CD8, and CD2 antibodies were purchased from BD Biosciences while anti-CD20 was supplied by Roche and anti-CD19 (FMC63) was kindly provided by the Department of Immunology at Flinders Medical Centre (Dr Peter Macardle). All antibodies were diluted in PBS to a working concentration of 200 μg mL^{-1}. A Cy3 labeled antibody (anti-goat IgG, Sigma) was used as a fluorescent locator dye on the microarrays. 30 μL aliquots of all factor dilutions were placed in 384-well (Nunc) source plates. A BioOdyssey Calligrapher (BioRad) was used for the contact printing of the microarrays. A solid pin print head (ArrayIt, SSP015, tip diameter 375 μm) was cleaned by sonication in MilliQ water for 10 min prior to printing. To avoid cross-contamination, pins were cleaned in PBS buffer solution containing 0.1% Tween-20 (Sigma), followed by rinsing in MilliQ water (18.2 MΩ cm) and drying (cycled thrice) between printing of each factor and each dilution. The printing chamber was held at 11 °C, and the humidity was kept at 65% during printing. After printing, the microarrays were stored at 4 °C for 48 h to allow the covalent antibody conjugation on the surface.

Blood collection and lymphocyte isolation

The collection of blood used for this study was approved by the Ethics Committee of CSIRO Food and Nutritional Sciences. Lymphocytes were isolated from whole blood samples by Ficoll-Paque (Amersham Pharmacia Biotech) gradient centrifugation methods previously described.[24] In short, fresh blood was collected by venipuncture into Vacutainer blood tubes with

lithium heparin anticoagulant (Greiner). Whole blood was diluted 1 : 1 with Hanks balanced salt solution (HBSS; Sigma) in 50 mL Falcon tubes. Blood was gently added onto Ficoll-Paque layer (1 : 3, v/v) and centrifuged at 400*g* for 30 min. The lymphocyte layer was removed and washed (1 : 3, v/v) in HBSS and centrifuged at 180*g* for 10 min. The supernatant was removed, and the pellet resuspended in HBSS (1 : 2, v/v) and centrifuged at 100*g* for 10 min. Again, the supernatant was removed and complete warmed (37 °C) medium (RPMI 1640 medium, Invitro Technologies, supplemented with 1% L-glutamine and 10% fetal bovine serum, 1% sodium pyruvate) was added and the cell density was adjusted to 1×10^6 cells per mL. Cell counts were performed using a Coulter Counter (Z1 Coulter Particle Counter, Beckman Coulter, USA).

Exposure of lymphocytes to ionizing radiation

The freshly isolated lymphocytes were exposed to γ-radiation with a CIS BIO International IBL 437 blood cell irradiator comprising of three stationary ^{137}Cs doubly encapsulated radiation sources emitting γ-radiation at 5.5 Gy min^{-1} at room temperature (22 °C). The exposure time was adjusted for replicate samples corresponding to 0, 1, and 2 Gy doses.

Culture of lymphocytes

For both the freshly isolated lymphocytes and the irradiated lymphocytes, cells were divided into 750 μL aliquots in separate culture tubes and PHA (Abbott Murex) was added for stimulation of nuclear division (final PHA concentration 30 μg mL^{-1}). Cells were incubated at 37 °C (5% CO_2, humid environment) for 44 h, after which, cytochalasin-B (Cyto-B, Sigma) was added to the cultures (final Cyto-B concentration 4.5 μg mL^{-1}) and incubated for another 27 h prior to transfer to the sorted cell microarrays.

Lymphocyte immobilization on the microarrays

Prior to incubation of cells with the microarrays, the arrays were soaked in PBS for 2 h to remove any excess (non-covalently bound) antibodies and quench the reactive epoxy groups on the surface of the substrates. The microarrays were then rinsed briefly with MilliQ water and dried under a stream of nitrogen. In order to minimize the required cell volumes, a wax pen (Dako) was used to define the perimeter of the arrayed antibodies. 27 h after Cyto-B addition, 1 mL of cell suspension was pipetted onto the microarray and incubated for 1 h at a density of $\sim 1 \times 10^6$ cell mL^{-1}. The supernatant was then removed, and the microarrays were gently rinsed with PBS to dislodge any unbound cells.

Cell fixation and staining

Microarrays. The cells were immediately fixed on the microarrays by first slightly swelling the lymphocytes by soaking (8 min) in a 0.56% (w/v) hypotonic solution of KCl (Sigma) in MilliQ water. The hypotonic solution was removed, and the microarrays were then soaked (10 min) in a prefixing solution consisting of a 1 : 1 mixture of NaCl (Sigma) solution (0.9% in MilliQ water, w/v) and a solution of methanol and acetic acid (5 : 1, v/v). After incubation in the prefixing solution, the microarrays were fixed in methanol and acetic acid (5 : 1, v/v, stored at −20 °C) for 10 min (3 times). The microarrays were dried in air for 30 min and stained with Diff Quik with moderate adjustments to the protocol from the supplier (Diff Quik kit, Lab Aids). The arrays were stained by dipping the arrays in Diff Quik orange stain #1 (6 times for 1 s per dip) followed by dipping in Diff Quik blue stain #2 (4 times for 1 s per dip) and then immediately rinsed in MilliQ water. The arrays were dried in air and coverslipped with Depex mounting media (Merck).

Cytospin of the non-sorted cells. For comparison to the cell microarrays, standard cytospin samples were prepared from non-sorted cells as described in detail elsewhere.[24] In summary, 80 μL of cell suspension was harvested onto microscope slides by a Shandon Cytospin centrifuge (Shandon Scientific Limited). The cells were then fixed and stained (with a Diff Quik kit) and the slides coverslipped with Depex.

Scoring of cell types and micronuclei in the CBMNcyt assay and scoring criteria used

The microarrays were analyzed with a Leica 20EB light microscope with 4×, 10×, 40×, and 100× (oil immersion) objectives. CBMNcyt assay biomarkers were analyzed at 1000× magnification. Both cytospin slides from standard heterogeneous non-sorted lymphocyte assays and microarray-sorted lymphocyte subsets were scored for the frequency of mononucleated, binucleated (BiN), multinucleated and MNi in BiN cells. For each CD antibody, 25 replicate spots were printed and cells residing on each individual spot were quantified and scored for each radiation dose (0, 1, and 2 Gy) to determine total cell attachment on the microarrays. The microarrays contained approximately 5000 viable cells for scoring per array and 3 microarrays in total were quantified (one microarray per dose of radiation). Statistical data were collected by combining CBMNcyt assay scores per row of arrayed antibody spots (5 spots per row) totaling 5 rows of each antibody (25 spots per antibody, as shown in the schematic in Fig. 2). In the cytospin standard assay samples, 500 BiN cells of the heterogeneous cell sample were scored per radiation dose with 3 replicate cytospin spots, as previously described.[24]

Statistical methods

A one-way ANOVA followed by a Tukey post-hoc test (Kaleidagraph software) was used to determine relevant statistical difference between the incidences of MNi within the lymphocyte subsets in comparison to the standard heterogeneous population (as prepared by CBMNcyt protocols). A one-way ANOVA followed by a Tukey post-hoc test was also used to determine significant difference between the percent cell attachment between the lymphocyte subsets at 0, 1, and 2 Gy exposure to γ-radiation and to determine significant differences of the cytostatic effects of γ-radiation between the subsets and the CBMNcyt standards.

Results and discussion

Fabrication of the microarray platform

An initial surface-design challenge for our microarray platform was to establish surface coatings that provide two primary functions: (1) inhibit non-specific cell attachment (for both adherent and non adherent cells), while also (2) providing reactive functional groups that allow the covalent attachment of monoclonal antibodies as capture probes. Physisorption of antibodies may be sufficient for many applications, but may fail under cell culture conditions. Antibodies or other biological factors covalently anchored to the substrate surface, therefore provide a more robust system under the relevant experimental conditions.

An allylamine plasma polymer was deposited in a radio-frequency glow discharge reaction on standard glass microscope slides. The resulting surface displayed amine functional groups, which were used to anchor subsequently spin-coated random copolymers made from GMA and poly(ethylene glycol) methacrylate.[33] To increase the stability of the coating, the spin-coated polymer was also crosslinked with a PEG diamine. The covalent immobilization of subsequently printed biomolecules on this surface was enabled by reactive epoxy groups present in the GMA component, while the display of poly(ethylene glycol) on the coating, provided by the PEGMA component, is known to inhibit non-specific cell attachment.[33] Nanolitre volumes of monoclonal antibodies were spotted onto these coatings with a robotic spotter (according to the process outlined in Fig. 1). This final step afforded an array of covalently bound and biologically active antibodies (for the print layout, see Fig. 2). The surfaces were stable under cell culture conditions for up to 7 days, and the cell attachment density was easily tuned by changing the incubation time and concentration of printed antibodies (ESI†, Fig. S1–S3).

Preparation of primary lymphocytes

Peripheral blood lymphocytes were isolated from human blood by Ficoll-Paque and density centrifugation[24] and then subsequently exposed to various levels of ionizing radiation at 0, 1, and 2 Gray (Gy) of γ-rays. Lymphocytic mitosis was stimulated by phytohaemagglutinin (PHA) approximately 2 h after exposure to radiation. Cytochalasin-B (Cyto-B) was added exactly 44 h after PHA activation to arrest the cells in the cytokinesis stage of cell division. At 27 h after Cyto-B addition, the heterogeneous lymphocyte population was incubated on the microarrays for 1 h for capture and sorting of the lymphocyte

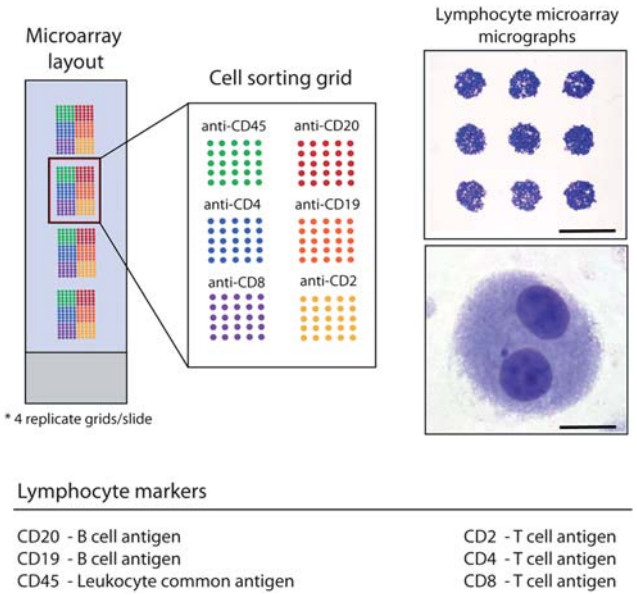

Fig. 2 A typical cell-sorting microarray platform with various CD antibodies displayed on surface-modified glass slides for immobilization of lymphocyte subsets. Lymphocytes were stained with Diff-Quik for imaging and scoring according to the CBMNcyt assay protocol. The microarrays provide *in situ* cell-sorting while also allowing for quantification of biomarkers for DNA damage. The printed monoclonal capture antibodies allow separation and immobilization of subsets of lymphocytes *via* their specific cell surface antigens. Scale bars represent 600 μm (top right micrograph of cell array) and 5 μm (bottom right micrograph of binucleated cell).

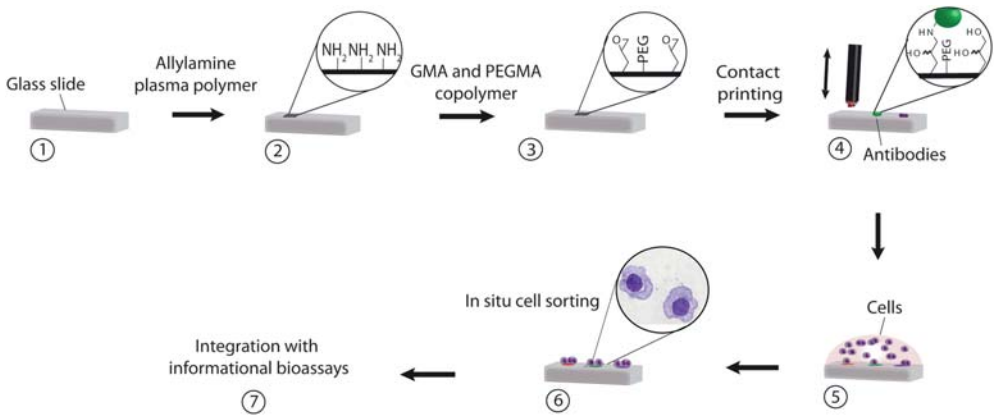

Fig. 1 Schematic of cell microarray fabrication. Glass slides were coated with an allylamine plasma polymer yielding an amine terminated surface. Subsequently, a copolymer of GMA and PEGMA was spin coated onto the slides providing reactive epoxy groups as well as PEG moieties to inhibit non-specific binding. Upon printing of capture antibodies, the epoxy groups on the surface underwent a ring opening reaction to form a covalent linkage with amine groups on the capture antibodies. The substrates were then rinsed thoroughly to remove any excess antibodies that were not covalently anchored. After 2 h incubation of the microarrays with a heterogeneous cell population, *in situ* cell sorting was complete.

subsets. Thereafter, all non-bound cells were removed by rinsing in PBS.

Specificity of cell sorting on the microarray platforms

Cell capture and spatial on-chip arrangement of lymphocytes into the various subpopulations were observed. Separate cell separation experiments were carried out to determine selectivity and specificity of the capture antibody probes on the microarray substrates (described in the ESI†). A purity of approximately 95% was achieved by cell sorting on the microarray (Fig. 3). The cells were fixed, stained (after performing modifications to the standard CBMNcyt assay protocol as described in Experimental methods section), and scored. We were able to score DNA damage in subsets of human lymphocytes by counting the frequency of occurrence of MNi (Fig. 4), while also concurrently investigating the cytostatic effects of γ-radiation on cell attachment for each of the subsets. Here, we measured the proportion of mononucleated, binucleated (BiN), and multinucleated cells and calculated the nuclear division index from these measurements.

Effects of radiation on cell attachment

The overall cell attachment after each dose of radiation was determined for each arrayed antibody spot (CD20, CD19, CD2, CD4, CD8, and CD45 antibodies; 25 replicate spots per antibody; Fig. 5). On the T cell capture antibodies (anti-CD2, anti-CD8, and anti-CD4), CD8+ cells (the notation used in this study follows the typical notation for flow cytometry and FACS, but we wish to point out the significant difference between the non-exclusive solution-based labeling techniques and the exclusive chip-based sorting) showed the most consistent cell attachment with relatively little difference in the number of cells attached after each dosage of radiation. At 0, 1 and 2 Gy radiation, 22%–27% of overall cell attachment (on the entire microarray) was observed on the anti-CD8 spots. CD4+ cells were attributed to 17–26% of overall cell attachment, and a slight reduction in cell attachment upon exposure to ionizing radiation was apparent, but was within the error margin. However, CD2+ cells that were exposed to 1 Gy and 2 Gy, showed an increase in cell attachment in comparison to the CD2+ cells that had not been exposed (from 10% of total cell attachment to more than 25%, $P < 0.0001$). Conversely, we observed a decrease of cells (from ~5% to ~2%, $P < 0.0001$) attaching to anti-CD19 arrayed spots after 2 Gy exposure. The change in percentage could possibly be attributed to an up- or down-regulation of surface antigens on the

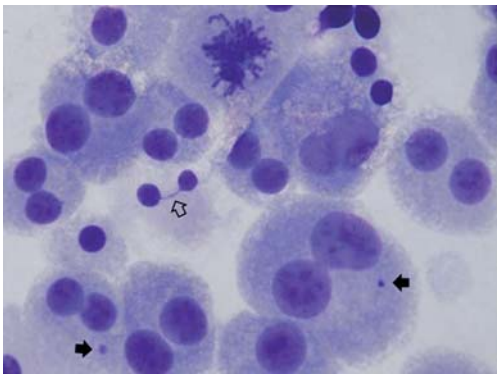

Fig. 4 Microscope images of cytokinesis-blocked lymphocytes on microarray CD2 spot (100× objective). Nucleoplasmic bridge (hollow arrow) and micronuclei (solid arrows) can be observed and quantified for the lymphocyte subsets. Cells are observed as mononucleated, binucleated or multinucleated cells. One cell in the top centre of the image is undergoing mitosis.

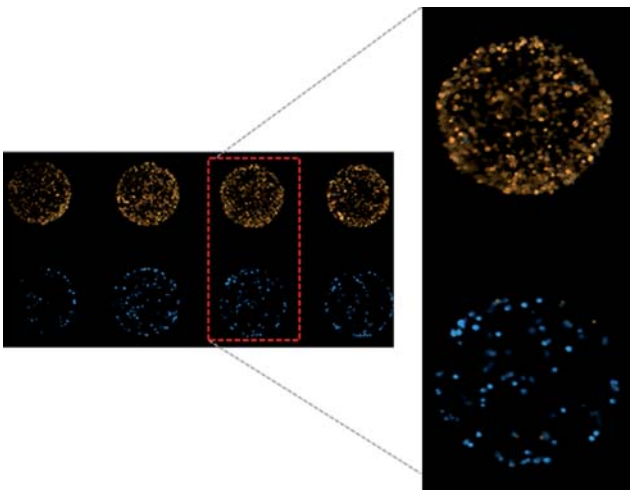

Fig. 3 *In situ* lymphocyte sorting into B and T cell subsets. A mixture of pre-stained B (HRIK, in blue, bottom row) and T cells (Jurkats, in orange, top row) were incubated on the microarrays for 2 h. After which, the cell suspension was washed off and only bound cells remained on the arrays. The subsets of cells were separated and immobilized onto spots displaying their respective antibodies, anti-CD20 (B cell antibody) and anti-CD2 (T cell antibody). The cell separation efficiency was determined to be ~95%.

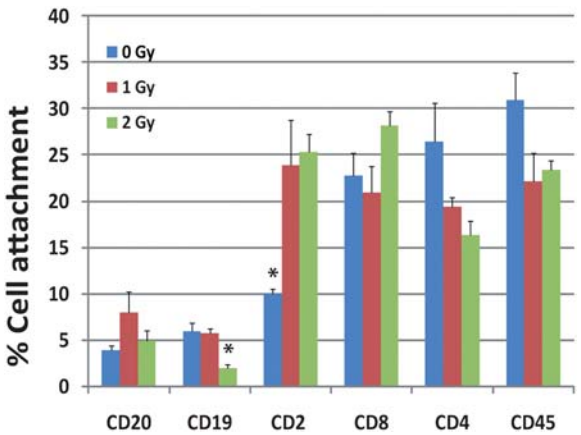

Fig. 5 Percent cell attachment on the microarrays divided into lymphocyte subsets. Cell attachment was quantified after various doses (0, 1, and 2 Gy) of ionizing radiation. The highest attachment was observed for the cells immobilized on the T cell capture antibodies (anti-CD2, anti-CD8, and anti-CD4) and the leukocyte antibody (anti-CD45). * Corresponds to statistically significant difference ($P < 0.0001$, $n = 5$) between the subsets comparing the doses of radiation exposure. The results indicate a down regulation of CD19 after 2 Gy exposure, and an up regulation of CD2 is observed on the microarrays after increasing doses of exposure.

lymphocytes when exposed to radiation; an effect which has been previously observed with other analytical methods.[35–37] This result suggests that we are able to monitor expression levels of cell surface antigens, and the microarray results agree with other methods.[36,37] Anti-CD45 was expected to yield high cell attachment since CD45 is a cell surface marker for both B and T cells. Indeed, cell attachment observed for arrayed anti-CD45 on the microarray substrates was observed to be between 22 and 31% of overall cell attachment on the microarrays, the highest average overall percent cell attachment. Apart from the anti-CD2 spots and anti-CD19, there were no significant differences in overall lymphocyte attachment for 0, 1, and 2 Gy radiation on any other portion of the microarrays.

Comparison between microarray and flow cytometry data

We compared the distribution of lymphocyte subsets in the lymphoid population by flow cytometry phenotyping (ESI† Fig. S4) to the percent attachment of the subsets on the microarrays (Fig. 5). There were notable differences between the two methods, particularly for the T cell capture antibodies (CD2, CD8, and CD4). We observed lower proportions of cells attached to anti-CD2 spots than those that were phenotyped as CD2+ by flow cytometry. Conversely, the anti-CD8 and anti-CD4 antibodies captured higher proportions of T cells than observed as CD4+ or CD8+ by flow cytometry. The discrepancies between the cell microarray and the flow cytometry results are not surprising considering the conceptual and experimental differences between a surface capture-based phenotyping where a cell can only attach to one antibody spot (exclusive capture) and the flow cytometry approach, where multiple phenotypic markers can be identified simultaneously for each cell (non-exclusive labeling). Due to the considerable differences in methodologies of the two separation techniques, a direct and quantitative comparison cannot be accurately stated. Flow cytometry defines the lymphocyte sub-populations as a percent of total CD45 positive lymphoid cells. The capture system defines the subpopulations as the percentage of lymphoid cells captured on an individual spot as a proportion of the total number of cells captured on all spots. Hence the capture system will reflect not only the proportion of cells able to be captured but also intrinsic differences in the affinity of the capture antibodies and in the antigen density on the surface of the particular lymphocyte subset.

With flow cytometry, we did not observe significant differences in percentage of subsets present after varying doses of radiation (ESI†, Fig. S4), contrary to the results obtained on the microarrays (Fig. 5). Radiation induced up- or down-regulation of surface antigens may not necessarily be observed with flow cytometry.[36,37] For example, whilst increases in expression of CD2 on a cell already expressing CD2 as well as CD4 and CD45 will not affect the phenotyping of this cell by flow cytometry, it may well affect cell attachment on the microarray and in particular may result in cell attachment on anti-CD2 spots rather than anti-CD4 or anti-CD45 spots.

Mitotic stimulation

Besides identifying specific subsets of lymphocytes, we were also able to determine which subsets responded more efficiently to PHA stimulation by determining the percentage of mononucleated, binucleated (BiN) and multinucleated cells for the three chosen levels of ionizing radiation and for the six subsets of lymphocytes identified by the microarray (Table 1). We observed differences in a few particular subsets in comparison to the cytospin standards, particularly for the mononucleated cells at 1 Gy and 2 Gy and in some cases for BiN and multinucleated cells. However, the most notable difference was observed with mononucleated cells attaching to anti-CD20. The total number of mononucleated cells (73.1 ± 5%) was

Table 1 Cytostatic effects of radiation exposure on PHA stimulated lymphocytes subsets. The percentage of mono-, bi-, and multi-nucleated cells were calculated for each lymphocyte subset and the effects of radiation on mitotic stimulation were studied. Immediately after isolation of lymphocytes from whole blood, the cells were exposed to 0, 1, 2 Gy doses of ionizing radiation. Mitotic cell division was stimulated by PHA for 44 h and blocked with cytochalasin B. After incubation of the heterogeneous mix of cells on the arrays, the immobilized cells on their corresponding capture antibody were counted and the percentage of mono-, bi-, and multi-nucleated cells were determined per arrayed antibody. This was carried out on the microarrays (25 arrayed spots per antibody for each dose of radiation) and the cytospin standard samples are included for comparison. The nuclear division index (NDI) for the subsets was also determined. * Corresponds to statistically significant difference, $P < 0.0001$

Subset	0 Gy				1 Gy				2 Gy			
	% Mono	% Bi	% Multi	NDI	% Mono	% Bi	% Multi	NDI	% Mono	% Bi	% Multi	NDI
CD20	52.1 ± 5	45.6 ± 6	2.2 ± 3	1.5	*58.1 ± 5	40.0 ± 5	1.4 ± 1	1.4	*73.1 ± 5	25.9 ± 5	1.0 ± 2	1.3
CD19	55.9 ± 5	42.4 ± 6	1.7 ± 1	1.5	*57.4 ± 2	41.5 ± 2	1.0 ± 1	1.5	57.0 ± 6	43.0 ± 6	*0 ± 0	1.4
CD2	45.6 ± 2	52.8 ± 2	1.7 ± 1	1.6	*59.1 ± 3	*36.7 ± 3	*4.2 ± 1	1.5	*50.9 ± 4	41.9 ± 4	7.2 ± 3	1.6
CD8	45.4 ± 4	50.3 ± 2	4.3 ± 2	1.6	51.3 ± 1	39.3 ± 2	9.5 ± 1	1.8	52.2 ± 2	40.7 ± 4	7.1 ± 3	1.6
CD4	43.4 ± 3	53.1 ± 3	3.4 ± 1	1.6	55.1 ± 2	39.6 ± 2	5.2 ± 2	1.5	59.2 ± 8	38.5 ± 9	2.3 ± 2	1.4
CD45	49.6 ± 2	45.3 ± 1	5.1 ± 2	1.6	52.7 ± 3	41.1 ± 2	6.1 ± 2	1.6	59.8 ± 6	36.6 ± 6	3.6 ± 1	1.5
Cytospin	44.9 ± 4	47.7 ± 4	6.9 ± 1	1.6	51.8 ± 4	40.4 ± 3	7.8 ± 1	1.6	51.1 ± 2	40.1 ± 4	9.0 ± 1	1.6

significantly higher ($P < 0.0001$) than for the cytospin standard and cells attaching to anti-CD2 portion of the arrays after 2 Gy radiation exposure, which gave rise to a lower value of BiN cells (25.9 ± 6%, $P < 0.05$) for CD20+ cells. This could imply that these cells are somehow hindered from undergoing mitosis, possibly due to a more stringent cell cycle checkpoint arrest of nuclear division or alternatively cells with DNA damage are prevented from completing nuclear division.[38] Our results therefore suggest that differences in susceptibility to ionizing-radiation-induced chromosome damage may exist between subsets of B and T lymphocytes.

The nuclear division index (NDI) was also calculated for the subsets. This value relates to the proliferative status of viable cells and is an important quality control measure indicative of successful lymphocyte culture and of mitogenic response. The latter is known to decline with age and suppressed immune response.[24] The NDI was calculated for 0, 1, and 2 Gy dosed samples on both the microarrays and the standard cytospin samples. There were no significant differences in NDI values between the subsets (Table 1) or the heterogeneous samples. The values ranged from 1.4–1.7 for the sorted cell microarrays while the standard heterogeneous samples remained constant at 1.6. These results are consistent with the literature showing that radiation exposure does not substantially influence NDI of lymphocytes.[39]

CBMNcyt assay on heterogeneous mixture of non-sorted lymphocytes

The CBMNcyt assay has been used extensively to assess effects of various factors including ionizing radiation, cytotoxic agents, environmental, nutritional, and age-related factors on heterogeneous mixtures of human lymphocytes.[30,40,41]The cytokinesis-blocked heterogeneous populations of human primary lymphocytes were fixed to slides *via* the cytospin method and scored for MNi content according to the standard CBMNcyt assay protocols.[24] The MNi frequency was determined per 500 BiN cells (with a sample replicate of 3, Fig. 6). The percentage of the MNi content in BiN cells of the standard samples without any exposure to ionizing radiation was 1.0 ± 0.2%. Upon increasing exposure of γ-radiation, we observed an increase in MNi content to 2.8 ± 0.7% for 1 Gy ($P = 0.005$) and to 13.4 ± 3.3% frequency of MNi after 2 Gy dose ($P = 0.0018$). Specific subset behavior upon exposure to ionizing radiation or other factors has not been extensively studied with the CBMNcyt assay due to the requirement of additional efforts for alternative cell separations.

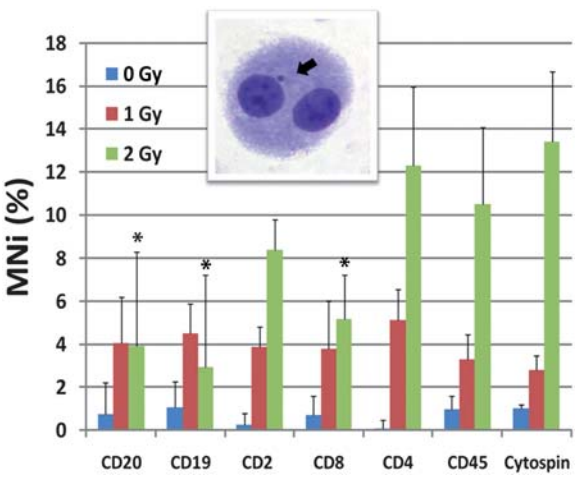

Fig. 6 Frequency of MNi (black arrow) within lymphocyte subsets after radiation exposure of 0, 1, and 2 Gy as determined on the microarrays. Increasing doses of radiation lead to an increase in the frequency of MNi in the cells. The largest difference between 0 Gy and 2 Gy doses was observed on T cell capture antibodies including CD2, CD4, and CD45 antibodies. * Corresponds to statistically significant difference ($P < 0.05$) of the frequency of MNi of the subsets in comparison to the cytospin standard (heterogeneous lymphocyte sample). 500 BiN cells were scored per cytospin standard (with 3 replicates) and approximately a total of 5000 cells per microarray were scored (for each radiation dose).

CBMNcyt assay on sorted cell microarrays

Unlike the standard CBMNcyt methods that measure the genetic damage across a heterogeneous population, we were able to separate lymphocytes into their respective subsets and measure genomic instability within lymphocyte subsets concurrently by means of the CBMNcyt assay on the chip. Each subset on the microarray was scored according to the CBMNcyt protocol.[24] The number of MNi increased as the radiation dose increased for cells binding to anti-CD2, anti-CD8, anti-CD4, and anti-CD45 spots (Fig. 6). For the B cells, an increase in the frequency of MNi present was observed for CD20+ and CD19+ subsets from 0 Gy to 1 Gy, but no further increase in MNi from 1 Gy to 2 Gy (Fig. 6). The lymphocyte subsets that appeared to be most affected by ionizing radiation were the T cells, CD2+ and CD4+ suggesting that these cells show an increased propensity to accumulate chromosome damage upon exposure to ionizing radiation and remain mitotically active. CD2+ cells demonstrated an increase in frequency of MNi from <0.3% for 0 Gy to 8.9% MNi after 2 Gy exposure. CD4+ cells showed the largest increase in MNi detection ranging from <0.1% for 0 Gy to 12.3% MNi frequency after 2 Gy ($P < 0.0001$). CD45+ cells also showed a significant difference after 2 Gy of radiation in comparison to 0 Gy exposure. CD45+ cells yielded values similar to the heterogeneous non-sorted samples (cytospin prepared standards). This was expected since CD45 is a leukocyte marker (and is expressed on all B and T cell subsets). In comparison to the standard cytospin samples, we observed a few significant differences in the frequency of MNi present in specific subsets upon increasing levels of exposure to ionizing radiation. The most significant differences were observed in the B cells captured by anti-CD20 and anti-CD19. These B cells had a lower frequency of MNi present than the heterogeneous non-sorted mix of lymphocytes after 2 Gy exposure (~3 to 4% *versus* ~13% respectively; $P < 0.05$). Similarly, CD8+ cells demonstrated lower levels of MNi frequency (~5% after 2 Gy) compared to the non-sorted standard. In the case of cells captured by anti-CD20, these differences could be explained by nuclear division inhibition of damaged cells given their slightly reduced NDI (1.3) and their low % BiN cell frequency (~26%) following 2 Gy exposure (Table 1).

Conclusions

We demonstrate a sorted cell microarray platform, which not only allows for facile cell separation and phenotyping but is at the same time compatible with quantitative sub-cellular analysis and informational cell-based assays. Other cell separation techniques such as FACS, MACS or differential plating/panning methods cannot be combined with cell-based assays *in situ* and need to be performed separately. While these techniques are generally regarded as efficient methods to yield high cell purity, they often consume large volumes of cell marker reagents (specifically for differential plating), and the cell numbers required often limit sample throughput. In contrast, the microarray format prints nanolitre scale volumes of reagents and can be expanded into high density formats for high-throughput analysis.

In particular, our on-chip cell-sorting platform is capable of quantifying the extent of genetic damage within specific subsets of human primary lymphocytes by means of the CBMNcyt assay. This strategy allows the identification of specific cellular subsets that are more susceptible to cyto- and genotoxic events induced by factors such as exposure to ionizing radiation. Our study is of course only of proof-of-principle nature. However, if our findings are validated in a clinical study, this would have significant impact on the bone marrow therapy of persons exposed to ionizing radiation.

Beyond this particular assay, the approach presented paves the road for the adaptation of a raft of cell-based assays or combinations of assays including calcium signaling, protein localization, toxicology, gene expression or knock-down, apoptosis and receptor activation to the microarray format.[42–44] The on-chip, high-content cytometric bioassay format presented here is conducive to a more comprehensive, systems-level understanding of cells, their involvement in disease and finally development of possible targets for therapy benefiting the fields of diagnostic, therapeutic, and preventative health technologies.

Competing interests statement

The authors declare that they have no competing financial interests.

Acknowledgements

The authors would like to thank Maurizio Ronci and Caroline Bull for helpful discussions. This work was supported by the CSIRO Flagship Collaboration Fund. E.J.A. designed and performed experiments, contributed blood, analyzed data, and prepared manuscript; C.S. collected blood and advised on cell biology; S.B. performed FACS analysis and supplied antibodies; M.H. advised on cell biology; P.M. supplied antibodies, analyzed and interpreted data, edited paper; M.F. conceived the idea of using the CD antibody microarrays for cell sorting of cytokinesis-blocked lymphocyte subsets and then to score the CBMNcyt biomarkers on the microarray-sorted cells, analyzed data, and edited paper; H.T. contributed to experimental design, analyzed data, and edited paper; N.H.V. supervised project, designed experiments, analyzed data, and prepared manuscript.

References

1 J. J. Diaz-Mochon, G. Tourniaire and M. Bradley, *Chem. Soc. Rev.*, 2007, **36**, 449–457.
2 J. M. Schwenk, O. Poetz, S. Kramer and T. O. Joos, *Bioforum*, 2003, **26**, 717–719.
3 D. B. Wheeler, A. E. Carpenter and D. M. Sabatini, *Nat. Genet.*, 2005, **27**, S25–S30.
4 D. Castel, A. Pitaval, M. A. Debily and X. Gidrol, *Drug Discovery Today*, 2006, **11**, 616–622.
5 D. S. Chen and M. M. Davis, *Curr. Opin. Chem. Biol.*, 2006, **10**, 28–34.
6 S. N. Bailey, D. M. Sabatini and B. R. Stockwell, *Proc. Natl. Acad. Sci. U. S. A.*, 2004, **101**, 16144–16149.
7 M.-Y. Lee, R. A. Kumar, S. M. Sukumaran, M. G. Hogg, D. S. Clark and J. S. Dordick, *Proc. Natl. Acad. Sci. U. S. A.*, 2008, **105**, 59–63.
8 I. S. Baird, A. Y. Yau and B. K. Mann, *Biotechniques*, 2008, **44**, 249–255.
9 C. J. Flaim, S. Chien and S. N. Bhatia, *Nat. Methods*, 2005, **2**, 119–125.
10 D. G. Anderson, S. Levenberg and R. Langer, *Nat. Biotechnol.*, 2004, **22**, 863–866.
11 G. H. Underhill and S. N. Bhatia, *Curr. Opin. Chem. Biol.*, 2007, **11**, 357–366.
12 E. J. Anglin, R. Davey, M. Herrid, S. Hope, M. Kurkuri, P. Pasic, M. Hor, M. Fenech, H. Thissen and N. H. Voelcker, *Cytometry, Part A*, 2010, **77A**, 881–889.
13 A. L. Hook, D. G. Anderson, R. Langer, P. Williams, M. C. Davies and M. R. Alexander, *Biomaterials*, 2010, **31**, 187–198.
14 Y. Mei, S. Gerecht, M. Taylor, A. J. Urquhart, S. R. Bogatyrev, S. W. Cho, M. C. Davies, M. R. Alexander, R. S. Langer and D. G. Anderson, *Adv. Mater.*, 2009, **21**, 2781–2786.
15 L. Belov, O. de la Vega, C. G. dos Remedios, S. P. Mulligan and R. I. Christopherson, *Cancer Res.*, 2001, **61**, 4483–4489.
16 L. Belov, P. Huang, J. S. Chrisp, S. P. Mulligan and R. I. Christopherson, *J. Immunol. Methods*, 2005, **305**, 10–19.
17 H. Zhu, M. Macal, C. N. Jones, M. D. George, S. Dandekar and A. Revzin, *Anal. Chim. Acta*, 2008, **608**, 186–196.
18 M. Berwick and P. Vineis, *J. Natl. Cancer Inst.*, 2000, **92**, 874–897.
19 S. Gutiérrez-Enríquez and J. Hall, *Mutat. Res., Genet. Toxicol. Environ. Mutagen.*, 2003, **535**, 1–13.
20 N. Watanabe, H. Kanegane, S. Kinuya, N. Shuke, K. Yokoyama, H. Kato, G. Tomizawa, M. Shimizu, H. Funada and H. Seto, *J. Nucl. Med.*, 2004, **45**, 608–611.
21 I. Decordier, A. Papine, G. Plas, S. Roesems, K. Vande Loock, J. Moreno-Palmono, E. Cemeli, D. Anderson, A. Fucic, R. Marcos, F. Soussaline and M. Kirsch-Volders, *Mutagenesis*, 2008, **24**, 85–93.
22 D. Varga, T. Johannes, S. Jainta, S. Schuster, U. Schwartz-Boeger, M. Kiechle, B. Patino Garcia and W. Vogel, *Mutagenesis*, 2004, **19**, 391–397.
23 P. Smolewski, Q. Ruan, L. Vellon and Z. Darzynkiewics, *Cytometry, Part A*, 2001, **45**, 19–26.
24 M. Fenech, *Nat. Protocols*, 2007, **2**, 1084–1104.
25 P. Thomas, N. J. O. Callaghan and M. Fenech, *Mech. Ageing Dev.*, 2008, **129**, 183–190.
26 L. Petrozzi, C. Lucetti, R. Scarpato, G. Gambaccini, F. Trippi, S. Bernardini, P. Del Dotto, L. Migliore and U. Bonuccelli, *Neurol. Sci.*, 2002, **23**, S97–S98.
27 R. A. El-Zein, M. B. Schabath, C. J. Etzel, M. S. Lopez, J. D. Franklin and M. R. Spitz, *Cancer Res.*, 2006, **66**, 6449–6456.
28 D. Scott, J. B. Barber, E. L. Levine, W. Burrill and S. A. Roberts, *Br. J. Cancer*, 1998, **77**, 614–620.
29 P. Thomas, S. Harvey, T. Gruner and M. Fenech, *Mutat. Res.*, 2008, **638**, 37–47.
30 M. Fenech, *Mutagenesis*, 2005, **20**, 255–269.
31 M. Fenech, *Health Phys.*, 2010, **98**, 234–243.
32 H. Thissen, G. Johnson, G. McFarland, B. C. H. Verbiest, T. Gengenbach and N. H. Voelcker, *Proc. SPIE*, 2006, **6413**, 64130B1–64130B9.
33 M. D. Kurkuri, C. Driever, G. Johnson, G. McFarland, H. Thissen and N. H. Voelcker, *Biomacromolecules*, 2009, **10**, 1163–1176.
34 M. D. Kurkuri, C. Driever, H. W. Thissen and N. H. Voelcker, *Proc. SPIE*, 2006, **6413**, 64130Z1–64130Z12.
35 C. Sambani, H. Thomou and P. Kitsiou, *Int. J. Radiat. Biol.*, 1996, **70**, 711–717.

36 H. Tuschl, R. Kovac and A. Wottawa, *Int. J. Radiat. Biol.*, 1990, **58**, 651–659.
37 M. J. Pecaut, G. A. Nelson and D. S. Gridley, *In vivo*, 2001, **15**, 195–208.
38 M. Allday, G. Inman, D. Crawford and P. Farrell, *EMBO J.*, 1995, **14**, 4994–5005.
39 M. Fenech, S. Bonassi, J. Turner, C. Lando, M. Ceppi, W. Chang, N. Holland, M. Kirsch-Volders, E. Zeiger, M. Bigatti, C. Bolognesi, J. Cao, G. De Luca, M. Di Giorgio, L. Ferguson, A. Fucic, O. Lima, V. Hadjidekova, P. Hrelia, A. Jaworska, G. Joksic, A. Krishnaja, T. Lee, A. Martelli, M. McKay, L. Migliore, E. Mirkova, W. Müller, Y. Odagiri, T. Orsiere, M. Scarfì, M. Silva, T. Sofuni, J. Surralles, G. Trenta, I. Vorobtsova, A. Vral and A. Zijno, *Mutat. Res.*, 2003, **534**, 45–64.
40 C. Torres de Lemos and B. Erdtmann, *Mutat. Res.*, 2000, **467**, 1–9.
41 I. Sari-Minodier, T. Orsiere, L. Bellon, J. Pompili, C. Sapin and A. Botta, *Mutat. Res.*, 2002, **521**, 37–46.
42 A. L. Hook, N. H. Voelcker and H. Thissen, *Acta Biomater.*, 2009, **5**, 2350–2370.
43 O. Rausch, *Curr. Opin. Chem. Biol.*, 2006, **10**, 316–320.
44 M. A. Debernardi and G. Brooker, *Methods Enzymol.*, 2006, **414**, 317–335.